HUNGARIAN UNIVERSITY OF AGRICULTURE AND LIFE SCIENCE

Performance and power quality evaluation of grid-connected solar photovoltaic systems

PhD Thesis

by

Divine Kafui Atsu

Gödöllő
2021

Doctoral school

Denomination: Doctoral School of Mechanical Engineering

Science: Mechanical Engineering

Leader: Prof. Dr. István Farkas, DSc
Institute of Technology
Hungarian University of Agriculture and Life Science,
Gödöllő, Hungary

Supervisor: Prof. Dr. István Farkas, DSc
Institute of Technology
Hungarian University of Agriculture and Life Science,
Gödöllő, Hungary

Co-Supervisor: Dr. István Seres, PhD
Institute of Mathematics and Basic Science
Hungarian University of Agriculture and Life Science,
Gödöllő, Hungary

………………………………   ………………………………
Affirmation of supervisor   Affirmation of head of school

CONTENTS

1. INTRODUCTION, OBJECTIVES

The growing penetration rate of solar PV into the grid significantly impacts the electric grid because of the variability of the energy source and the bidirectional power flow effect they introduce into the power network. The impact becomes more severe, especially in low voltage systems with low demand levels having high penetration levels. Utility providers have become sceptical in allowing the continuous connection of PV systems onto the grid, thus, heightening the awareness of power quality issues. Consequently, new power quality regulations and standards are being imposed by different countries and sub-regions to regulate power fed into the grid from distributed sources to ensure high grid power efficiency and stability.

This current research seeks to investigate the performance of microinverter and string inverter systems under steady irradiation supply (solar PV simulator) and outdoor ambient conditions. The power quality characteristic measurements for different scenarios will be analysed, and their compliance with available standards for grid-connected PV systems assessed. The harmonic current's dependence on the system harmonic voltage will also be investigated. The main aim of the research is to conduct a comprehensive investigation of the technical challenges and the impacts of integrating solar PV into the low voltage power distribution network. Emphasis will be laid on assessing the different systems' outputs by applying various inverters and working scenarios. Specific consideration will be given to the Hungarian grid operational conditions. The detailed research objectives are as follows:

- Determine the performance output of microinverters under constant indoor conditions and outdoor real operation condition.

- Investigate the performance output and compliance of microinverters under different outdoor working conditions and varying solar PV technologies.

- Assess the performance output of different grid-connected string inverters under varying ambient conditions and determine their compliance with specified grid-connection standards in the Hungarian low voltage power network.

- Determine the correlation between the harmonic current and the system harmonic voltage for the different inverter systems.

2. MATERIALS AND METHODS

This chapter presents the materials, procedures, and processes used in the research, including the scientific methods involved in the experiments and the description of the test systems to obtain the set research objectives.

2.1. Measurements with the solar PV simulator

This section of the study sought to analyse the quality of microinverters' power output by employing a solar PV simulator and modules of different technologies and make (structure) that meet the microinverter's requirements. The Geräte Unterricht Naturwissenschaft Technik (GUNT) ET255 set up was retrofitted to conduct the experiment as shown in Fig 1. An additional measuring point was created to enable the simultaneous measurement of the AC voltage and current using the power quality analyser. The switch-on voltage of the inverter is 35 V, and the MPP voltage tracking range lies between 28 V and 50 V. The PV generator's power output is 150 W, maximum Isc is 5.1 A, and maximum Voc is 41.3 V.
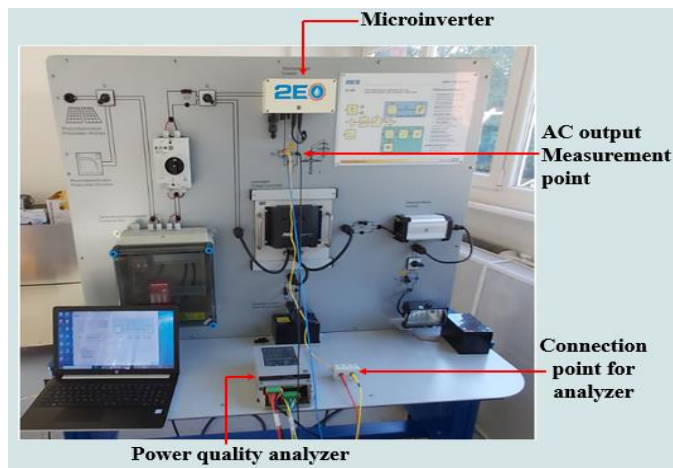

Fig. 1. Experimental setup

The initial test was conducted using the PV simulator as the PV power source to feed the inverter. Two scenarios were considered. Firstly, constant PV generation at fixed irradiation and temperature of 1000 Wm^{-2} and 25 °C, respectively. This selection generates a steady nominal power of 146 Wp, Voc of 41.3 V, Isc equals 5 A, Vmpp of 31.4 V, and Impp 4.65 A. The second scenario with the PV simulator as the PV power source applied irradiation of 400 Wm^{-2} at a constant module temperature of 25 °C, generating Voc of 39.6 V, Isc of 2 A Vmpp 32.3 V and Impp of 1.87 A. The peak power for the second scenario was 45 Wp.

The second investigation with the GUNT ET 255 employed PV modules in actual outdoor operation as the DC power source by using different module types. The Wally A3 electric power quality analyser with an in-built data logging capability was used to measure and store the AC output waveform characteristics. The measurements were computed over 10 to 12 cycles of consecutive windows, according to the IEC 61000-4-30 standard. Sampling was done synchronously with phase-locking at 512 samples/cycle with a range of 42.5 - 69 Hz (25.6 kHz @50 Hz). Solar radiation data was measured at the plane of the module or array (PoA) using the Delta – T SPN1 Pyranometer.

2.2. Evaluation of microinverter systems in outdoor operation

The study was undertaken at the forecourt of the Solar Energy and Environmental Engineering Laboratory in Szent Istvan University, Gödöllő, Hungary. The modules were fixed to an inclined support facing true south having an angle to the horizontal equal to the site's latitude. The installation of the modules is shown in Fig. 2. Measurements for each scenario were taken for ten hours (8 am-6 pm) in the second week of August 2020.

Fig. 2. Installed PV modules
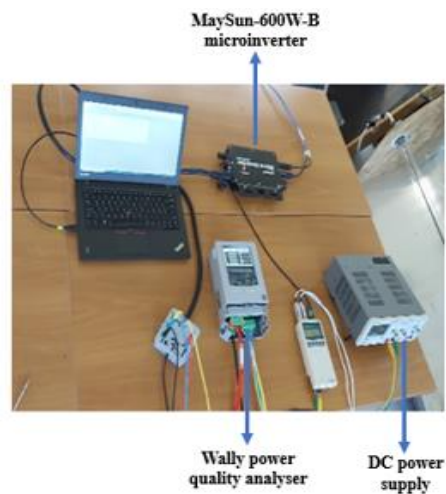
Fig. 3. Experimental setup for the microinverters

The next test was to investigate the performance of commercially available microinverters. The MaySun-600W-B (China inverter) and the GMI 300 (Holland inverter). The two main types of modules applied were the polycrystalline module (Solarex), and the monocrystalline modules (Juta). An extra measurement socket was built to connect the power quality analyser to the microinverter to enable the simultaneous measurement of both current and voltage. The setup is shown in Fig. 3.

2.3. Performance of grid-connected string inverter systems

Power quality assessment was conducted on the grid-connected solar PV system installed at Szent István University, Gödöllő, Hungary. The system is made up of two different PV technologies: Polycrystalline silicon (pc-Si) PV technology (ASE-100) and amorphous silicon (a-Si) PV technology (DS-40). It is divided into three sub-systems and installed on the flat roof of the student dormitory 'C' (47°35'45.4"N 19°21'51.7"E), as shown in Fig. 4. Sub-system 1 is connected to the SunPower SP3100-600 inverter, while sub-systems 2 and 3 are connected to the SunPower SP2800-550 inverter. Fig. 5 shows the photographic presentation of the measurement setup. Data on the various characteristics of the output signal was measured at intervals ranging from 200 ms to 6 s. Three days were selected from the lot to present contrasting outputs for low irradiation, steady and high irradiation, and intermittent solar radiation profiles.
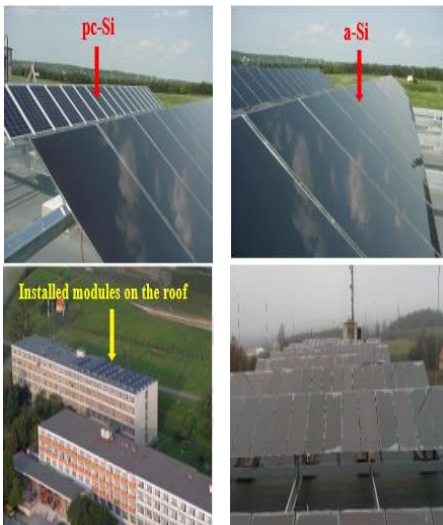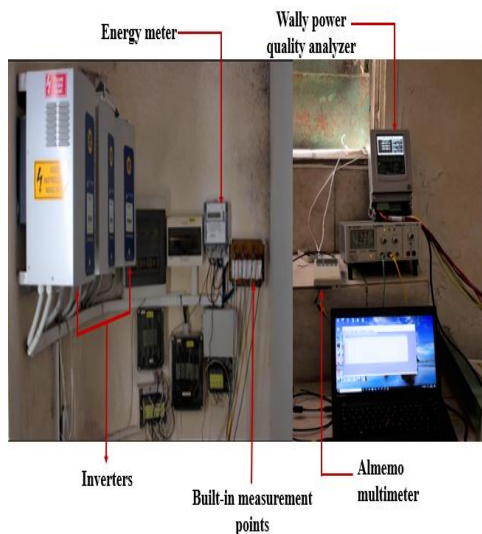

Fig. 4. Installed array on the rooftop   Fig. 5. Setup for the string inverters

3. RESULTS

This chapter presents the most important results obtained from the experimentation and their discussions.

3.1. Measurements with the solar PV simulator setup

3.1.1. Power factor for the indoor measurement

The power factor (cos ϕ) (PF) shows the phase angle between the current and the voltage signals of the AC output. It is generally expressed as a decimal or in percentage. Per the IEEE 1547 standard, solar PV grid-connected inverters are to be designed to operate at power factors close to unity. To comply with the standards, inverters are designed to suppress the reactive power to zero to achieve the abovementioned characteristic. The studied microinverter showed the same properties when the solar simulator (non-intermittent PV source) was used. The technical regulations concerning power factor for most countries specify that the power factor range at the point of common coupling should be ≥ 0.95, whether leading or lagging. The maximum power factors were 0.99502 and 0.99627 for the 400 Wm^{-2} and 1000 Wm^{-2}, and the minimum values were 0.9 and 0.9213 for 400 Wm^{-2} and 1000 Wm^{-2}, respectively. Throughout the study, the trend of power factor was all within the standard range except for four points within the study where the power factors were outside the prescribed scope, which may be due to some sudden losses. These occurred for both cases of 400 Wm^{-2} and 1000 Wm^{-2}, but at different times, as shown in Fig. 6.
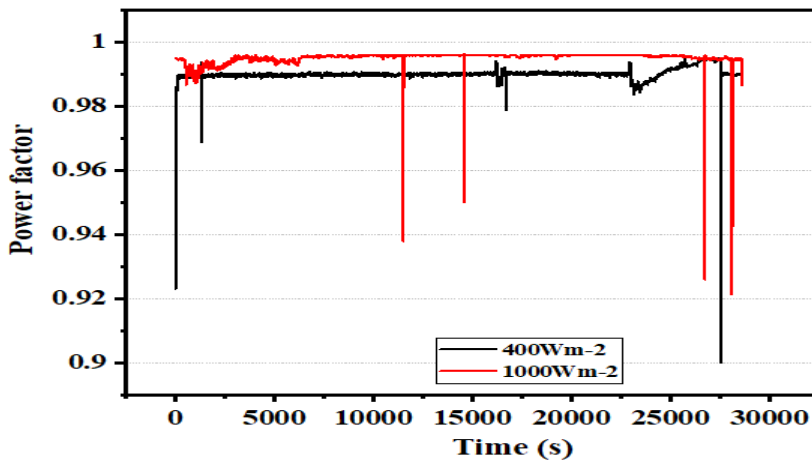

Fig. 6. Power factor profiles for 400 Wm^{-2} and 1000 Wm^{-2}

3.1.2. Power factor for the outdoor measurement

The power factor output of the microinverters in the outdoor operation depended significantly on the available irradiation as the power factor is derived from the values of the active power and the apparent power. This is an indication of the voltage and the current waveforms being out of phase. From the results, it could be seen that all three cases produced high percentages of values that were outside the specified limits.

Except for the case of the Solarex modules, the power factors plunged into the negatives for the other cases with the lowest power factors reaching -1.49 and -1.33, respectively, for Dunasolar and Juta modules. Comparing the results of the outdoor measurements to the study under the steady PV simulator, the power factor profiles recorded for all the cases studied using the solar simulator were within the standard limits, whiles the profiles for all the cases for the outdoor study had values that were outside the set limits. This points to the fact that unsteady solar radiation has a significant impact on the power factor profile. This was evident in the trend and correlation of the measured irradiation with the power factor profiles. The trends were similar for all three cases studied. The percentage of measured PF values below the standard limits for the cases studied were 67%, 54%, and 37% for Dunasolar, Juta, and Solarex module setups.

3.1.3. Current total harmonic distortion profiles

The results of the generated current total harmonic distortions (CTHD) for the studies with the solar simulator showed different trends compared to the results with the outdoor studies with the real solar modules, as presented in Fig. 7. It was observed that the CTHD output with the solar simulator (constant PV generation) was relatively steady with non-significant changes throughout the study. The CTHD generated in the outdoor studies with the microinverter had their minimum values at the start of the study. However, the trend changed with time; it began to increase for all three cases, even though the values were different for all the cases. The increase in the output for the Solarex, however, had a drastic upward change at about half past noon, after which it continued to increase linearly with time until the end of the study. It was evident the strong correlation between the drastic change in the current THD of the Solarex module with the trend of irradiation for the day. It was apparent that at the time of the change, there was an unstable solar radiation incident on the modules, and the intermittence continued until the end of the experimentation. The CTHD output for the Solarex was also the least from the start of the investigation until the point of the drastic increase at about noon when it rose above the results for the solar simulator but not above the results for the other outdoor investigations. The trend for the Dunasolar (a-Si frameless glass solar

module) increased continuously from its minimum value at the start of the study.
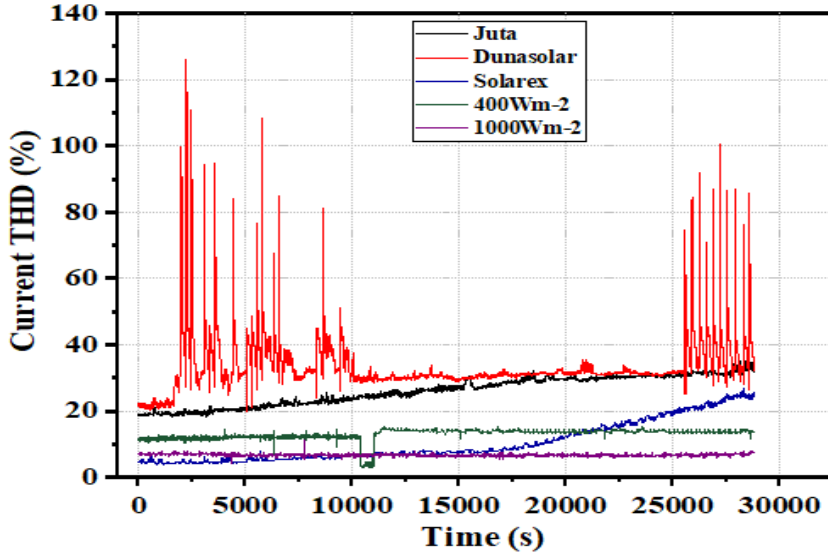

Fig. 7. Current THD for the studies with Juta, Dunasolar, Solarex, 400 Wm^{-2} and 1000 Wm^{-2}

It showed a unique behaviour during low and unsteady irradiation values. The CTHD increased drastically during such periods of irradiations, with values reaching as high as 126%. However, during periods of fairly steady solar irradiations, the generated CTHD for the Dunasolar was relatively stable.

3.2. Performance of commercial microinverters

This section presents the results and analyses the characteristic output of the different PV grid-connected microinverters (GMI 300 (Holland) and Maysun-600W-B (China)) using different sets of modules of various technologies under varying conditions in outdoor operation.

3.2.1. Power factor

With reference to the specified standards, the Holland microinverter with the Juta modules recorded a power factor profile with all its values below the set standard. The maximum and the minimum values recorded were 0.98 and -1.06, respectively, as presented in Fig. 8. The average power factor and the standard deviation were 0.796 and 0.14, respectively. However, the Holland microinverter with the Solarex set of modules had 0.398% of its power factor within the accepted range. The rest were below the 0.95 standard. The maximum and the minimum power factor were 0.98 and -1.056, respectively.

The standard deviation was 0.3915 for the Holland inverter, and Solarex set of modules.
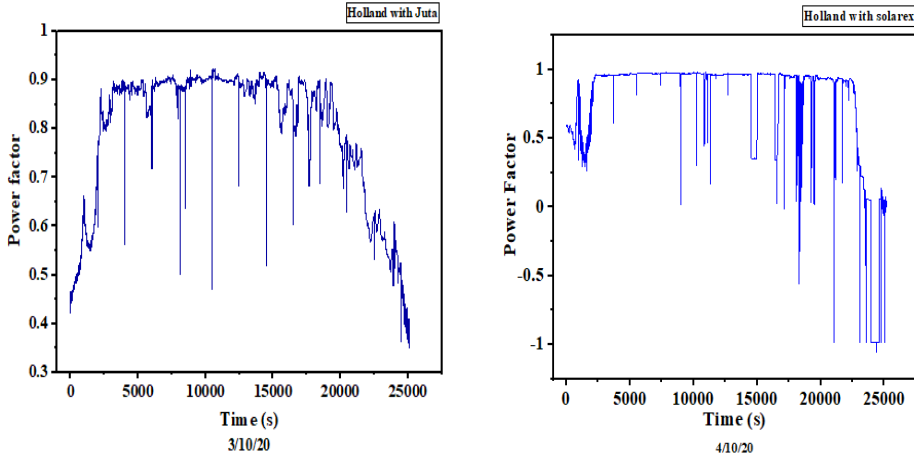
Fig. 8. Power factor profiles for Holland microinverter a) with Juta modules
b) with Solarex modules
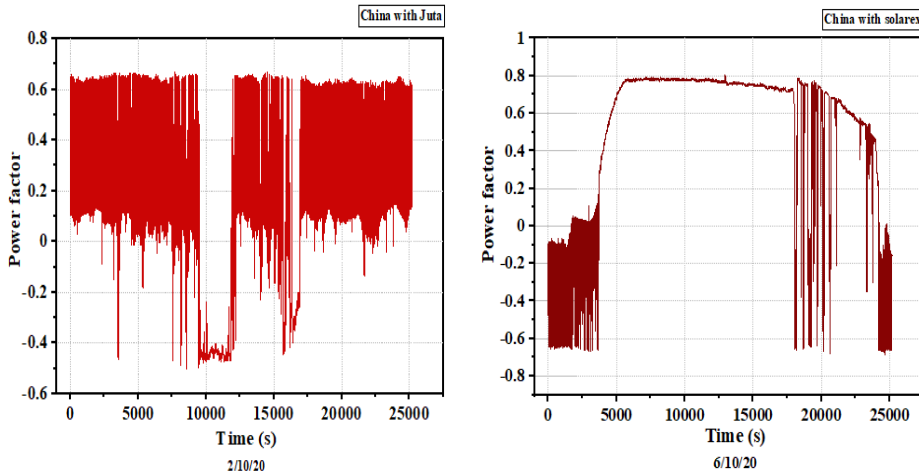
Fig. 9. Power factor profiles for China microinverter a) with Juta modules b)
with Solarex modules

The power factor recorded by the China microinverter in the studies conducted with the various set of modules were below the specified standard, which should be ≥0.95. The maximum and minimum PF recorded for the China microinverter were 0.67 and -0.5, and 0.8 and -0.69 for Juta and Solarex modules, respectively, as shown in Fig. 9. The average power factor and the deviation in PF values for the two setups were 0.09 and 0.287, and 0.52 and 0.373 for Juta and Solarex, respectively.

It is evident from the results that there was higher production of reactive power, especially for the China inverter with the Juta setup, causing the power factor to remain low and violating the specified standard for the greater part of the experimentation. It was observed that the China microinverter is integrated with an MPPT algorithm which suffers from the disadvantage of being slow in tracking especially if solar radiation had not been high and stable for an extended time. Due to this, the active power recorded was extremely low mainly in the negatives. This was evident in the results for the setup for the China inverter with Juta modules. Voltage-controlled MPPT could curtail the losses in power caused by dynamic tracking errors that would have occurred under intermittently changing solar radiation condition.

3.2.2. Current total current harmonic distortions

CTHD recorded for the test on the Juta modules (mc-Si) were higher than the results for the test on the Solarex (pc-Si) for both microinverters studied as shown in Fig. 9. Also, the CTHD for the China microinverter were higher than the CTHD for the Holland microinverter for the entire experimentation period for all the conditions studied. The Holland microinverter also recorded current THD that were beyond the limit with the Juta modules even though for the Solarex modules, except for 0.01% all the current THD recorded were beyond the specified limits.

It was observed that the THDs for the Solarex (pc-Si) were more stable over a prolonged period during the measurement compared to the results for the Juta (mc-Si) modules. The CTHD for the China microinverter were all beyond the specified standards. The Holland microinverter also recorded current THD that were beyond the limit for the Juta modules even though for the Solarex modules, except for 0.01% all the current THD recorded were beyond the specified limits. The high CTHD observed may be due to the presence of non-linearity of some components within the microinverter, which increase the current harmonics injected at the PCC.

The maximum and minimum current THD recorded for the Holland microinverter for the different sets of solar modules were 387.69% and 4.55%, and 147.79% and 5.24%, respectively for Solarex and Juta modules. The average current THD (CTHD) and the disparity in the recorded values in terms of standard deviation were 37.84% and 31.05, 65.82% and 10.95, respectively, for Solarex Juta modules. For the china microinverter, the maximum and minimum current THD were 291.82% and 57.44%, and 586.75% and 66.68%, respectively for Solarex and Juta modules.

The average CTHD and the standard deviations were 91.01% and 40.64, and 129.48% and 37.49, respectively for Solarex and Juta modules. The Holland

microinverter had lower deviations in CTHD compared to the China microinverter. The least variation of CTHD was however recorded for Holland microinverter with Juta module settings. It was observed that the CTHD fluctuates correspondingly to the intermittence of the solar radiation. The China microinverter suffered the disadvantage of slow tracking of the MPPT algorithm hence its inability to track the MPP at the instance of low solar radiation hence the widely unstable CTHD recorded for its measurement with the Juta modules. With similar irradiation levels recorded for the Holland inverter with Solarex and China inverter with Solarex, it has been found that the China inverter recorded a higher CTHD at the same period of high and stable solar radiation compared to the Holland inverter.

In the non-sinusoidal situations where voltages and currents contain harmonics. This equation provides an insight into the relationship between the true power factor and the CTHD. These two quantities are inversely proportional as shown in Eqn 1.

$$\text{PF} \approx \frac{\cos\varphi_1}{\sqrt{1+\text{THD}_i^2}}. \tag{1}$$

This also reveals that the higher the CTHD, the lower the PF. When there is no harmonic present, the power factor is equal to $cos\varphi_1$.

It has been observed that the CTHD for the China microinverter presented a unique relationship with the power factor profile recorded for both sets of experiments with Juta and Solarex solar modules. The output curves for the power factor and the CTHD were exactly inverse in shape or a reflection of each other in the horizontal plane, as shown in Fig. 10. This observation confirms the essence of Eq. 1. However, the inverse relationship between the power factor and the CTHD observed for the China microinverter was not evident in the results for the Holland microinverter. The correlation between low solar irradiation and the total harmonic distortions generated was apparent in the results for the China microinverter and the Juta setup, as shown in Fig. 10 and Fig. 11. It can, therefore, be said that Eq. (1) does not hold for all the inverters studied even under high irradiation levels.
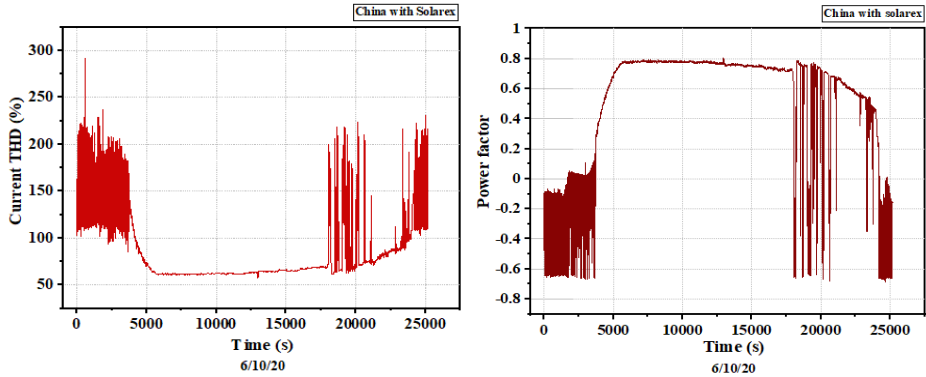
Fig. 10. Relationship between the power factor profile and the current total harmonic distortions of the China microinverter with Solarex
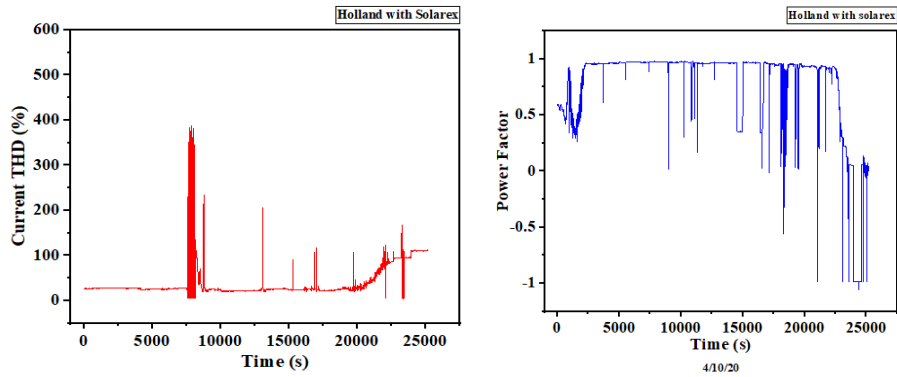

Fig. 11. Relationship between the power factor profile and the current total harmonic distortions of the Holland microinverter with Solarex

3.3. Power quality analysis of string inverter systems

3.3.1. Performance under high and steady solar radiation

This section presents the results and discussions for the study of the rooftop grid-connected PV system on the student dormitory of Szent Istvan University, Godollo – Hungary, for a day of high, steady and unintermittent solar radiation. Measurements were conducted for 10 hours (8 am – 6 pm). The various quantities were recorded at intervals ranging from 200 ms to 6 s.

3.3.1.1. Power factor

The power factor profiles for the three subsystems are presented in Fig. 12. The percentage of the power factor profiles of the various systems that violated the standards was 3.44%, 3.12% and 3.45%, respectively, for system 1, system 2 and system 3. The percentage of the power factor outside the specified standard (>0.95) was measured mostly in the latter period of the study when the irradiation levels were below 400 Wm^{-2} and decreasing. At the

initial stages of the study, even though the irradiation levels were below the 400 Wm^{-2}, but rising, that did not cause the power factor of the systems to fall below the 0.95 standard. The range of values for the recorded power factor for the different systems were 0.652 – 0.999, 0.265 - 0.998, and 0.651 – 0.999, respectively, for system 1, 2 and 3. The average values were 0.994, 0.991 and 0.993 for system 1, 2 and 3, respectively.
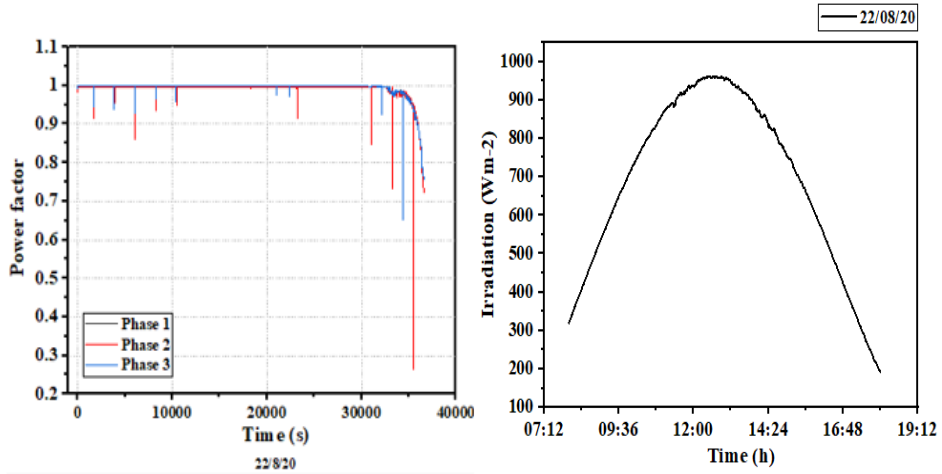

Fig. 12. a) Power factor profiles for the rooftop string inverter systems
b) Solar radiation profiles for high and non-fluctuating radiation

3.3.1.2. Current total harmonic distortions

The current total harmonic distortions (CTHD) profiles for the different rooftop systems have been presented in Fig. 13. Results show a few instances of relatively high instantaneous CTHDs spikes generated for all the phases that occurred at different times and were irrespective of the irradiation levels. The percentage deviation of these instantaneously high CTHDs from the steady values was 317% for phase 1, 480% for phase 2 and 640% for phase 3. The high CTHD observed maybe because of the presence of non-linearity of some components within the inverters, which increases the current harmonics injected at the PCC.

System 2 recorded the highest average current total harmonic distortion of 7.9% over the period. System 2 also recorded the highest standard deviation of 3.228, which indicates a high disparity in the measured CTHD for the system over the period compared to system 1 and 3. The maximum and minimum CTHDs for systems 1 and 3 are 37.56% and 3.68%, and 32.09% and 4.33%, respectively. The standard deviations for the various systems were 2.751, 3.228 and 2.709, respectively, for system 1, 2, and 3. The measured CTHDs for the different systems showed no correlation with the measured irradiation (whether low or high) for the period. The recorded CTHD profiles

15

increased linearly from the lowest values at the start of the investigations to the highest values at the end of the study.

With reference to the acceptable limits specified by the standards, it was observed that the percentage of the recorded CTHDs that violated the requirements were 32.7%, 12.5% and 16.4% for system 1, system 2 and system 3, respectively. This shows that with reference to the CTHDs, the severity of power quality issues recorded was greatest for system 1 compared to the results of the other systems. Comparably, system 2 recorded the least power quality issues in terms of the CTHD.
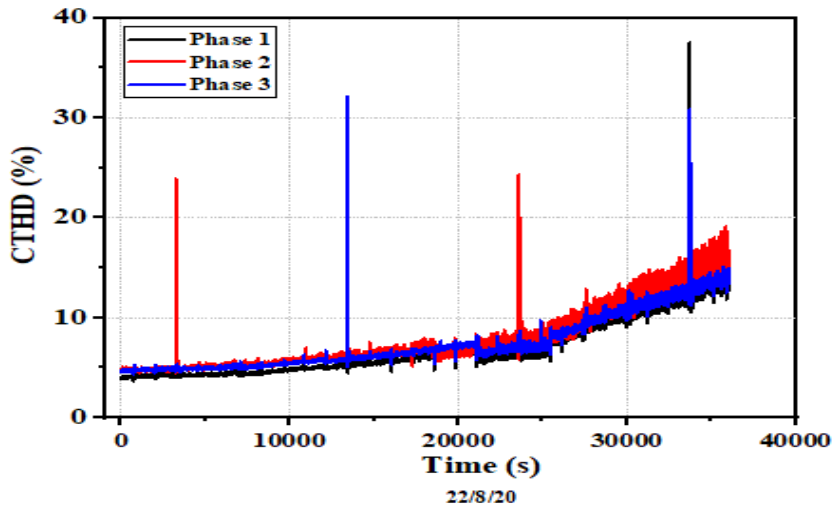
Fig. 13. Current total harmonic distortion for the three rooftop systems

3.3.2. Performance under intermittent low solar radiation

This section presents the results and discussions for the study on the rooftop grid-connected PV system for a day of sporadically high and low solar radiation. Measurements were conducted for 10 hours (8 am – 6 pm).

The current total harmonic distortions recorded for the three subsystems on a day of sporadically low and high solar radiation are presented in Fig. 14. Even though system 2 and 3 have the same configurations (inverter and array), the phase current and the output power of system 3, exceeded that of system 2 by about 5% throughout the study period. This was not an issue of shading or one set of array receiving less sunlight than the other set of the array, since the trend of 5% difference was observed from sunrise to sunset. This observation could result from the malfunctioning of one or some components in the balance of system. The lower the irradiation levels (approximately below 400 Wm^{-2}) irrespective of the intermittency, the increasing the CTHD. Even

though the intermittency was sporadic, at an intensity above 400 Wm^{-2}, the generated total harmonic distortions were relatively low and steady.

The CTHD for system 3 was higher than system1 and 2 throughout the study for the day. The maximum CTHDs were 77.2%, 62.7% and 77.7% for system 1, 2 and 3. The lowest CTHD of 4.2%, 4.1% and 4.7% for system 1, 2 and 3, respectively occurred at the start of the process. The highest continuous CTHDs were observed at the latter stages of the study when the irradiation levels were constantly decreasing and extremely low. It was seen that for system 3, only 2% of the recorded THD met the specified requirement. For system 1 and 2, 5.6% and 29.5% of the THD profile, respectively, was within the limits of the standards considered.
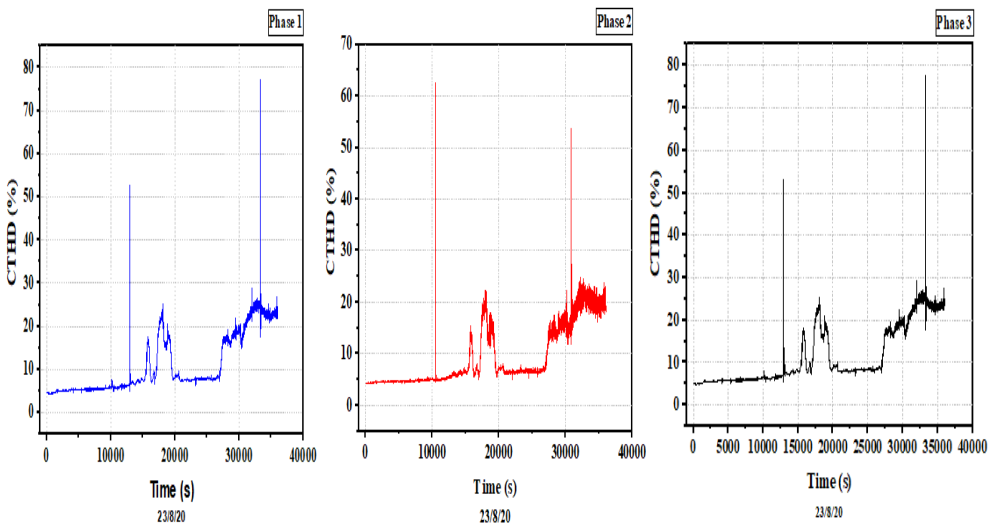

Fig. 14. Current total harmonic distortion for system 1, 2, and 3 on a day of high but intermittent solar radiation

3.4. Relationship between harmonic current and harmonic voltage

The correlation between the harmonic voltage and the harmonic current for each system and scenario studied was undertaken through detailed investigations. Data for days with high and steady solar radiation were chosen for the study. The regression analysis was used to determine the relationship by applying the least square method. Various scenarios with different datasets of 1000, and 3000 were applied. In further studies on the rooftop string inverter systems, data for the entire period was again used to compare the results with the other scenarios.

The test on the solar PV simulator (2E microinverter) with solar radiation set at 400 Wm^{-2} showed negative correlations for the $3^{rd,}$ and 7th harmonics while the 5th and the 9th harmonics recorded positive correlations. However, the test

with irradiation fixed at 1000 Wm^{-2} recorded a negative correlation for only the 7th harmonic whiles the correlations for the other harmonics were positive. Results showed varying correlations for the two scenarios under the constant irradiation conditions. Results for the string inverters showed that regardless of the system studied and the quantity of data used for the analysis, the correlation for the 5th harmonic remained positive, as was realized for the microinverters. The usage of 1000 and 3000 data points produced similar correlations for the 5th and the 7th harmonic orders for all the systems. The study with the 3000 data points had the same correlations for three harmonic orders for all the systems studied. Inferentially, it has been observed that the correlation is determined by the conditions prevailing and the harmonic order. Except for the 5th harmonic order, which showed a positive correlation for all the scenarios studied for both the string inverter systems and the microinverter systems, the trend for the other harmonic orders varied depending on the prevailing conditions. A plot of harmonic current against the harmonic voltage for the rooftop system is shown in Fig. 15.

A linear model for the relationship between the harmonic current and the harmonic voltage for the 5th harmonic order of microinverter systems and string inverter systems employed in low voltage grid systems has been established out of the results of the regression analysis as

$$I_H = 0.03979 + 0.0064 \; V_H,$$

where I_H is the harmonic current generated by the harmonic order and V_H is the harmonic voltage. The standard deviation was determined to be 0.0011.

Current harmonics are the main causes of voltage harmonics. The voltage source will be distorted by current harmonics due to the source impedance. If the source impedance of the voltage source is small, current harmonics will cause proportionally small voltage harmonics. There are occasions where the increase of harmonic current correlate to an increase in harmonic voltage. This can be explained by the lower values of energy being produced by the PV plant, and due to the changed relative impedance presented to the supply network, the contribution of 5th harmonic voltage by the supply system dominates. Hence, the positive correlation observed for the 5th harmonic order irrespective of the system type and operating condition.
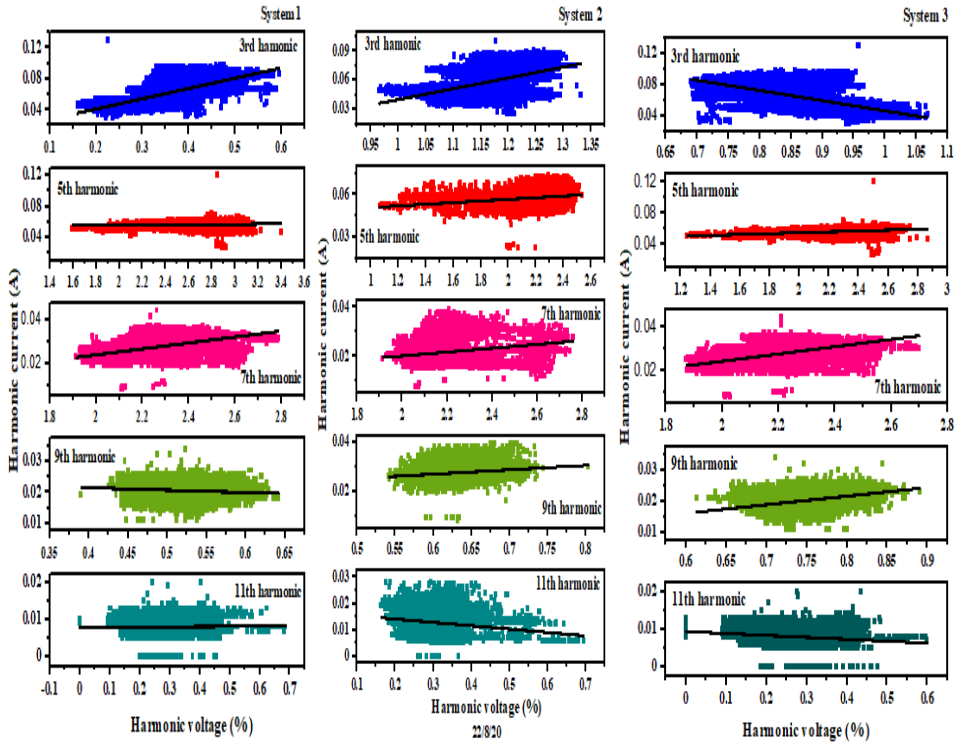
Fig. 15. Plots of harmonic current against system harmonic voltage for the rooftop string inverter systems (System 1, 2, and 3)

4. NEW SCIENTIFIC RESULTS

This section presents the new scientific findings from the research as follows:

1. Correlation between the power factor and the current total harmonic distortions

I have established that the inverse rule for the power factor and the current total harmonic distortions (CTHD):

$$PF_{true} \leq PF_{dist} = \frac{1}{\sqrt{1+(THD_I/100)^2}},$$

does not hold for all inverter systems under different operating conditions. It has also been determined that high power factor ≥ 0.95, within the acceptable standards depended on solar radiation values ≥ 400 Wm^{-2} or at $\geq 38\%$ the solar PV system's nominal capacity power generation and non-intermittency. I have also proven that irradiation levels below 400 Wm^{-2} or PV power generation less than $< 38\%$ of the nominal PV system rated capacity has the most significant negative impact on the power quality of the solar PV systems.

2. Current harmonic distortions by PV systems

In the case of the current total harmonic distortions generated by the different systems, I have ascertained that the microinverter systems did not meet the specified standard requirement of $<5\%$ of CTHD injection for all scenarios and conditions studied. I have proven that microinverters under outdoor conditions, generate the highest CTHD ranging from 14.3% to 129.5%. Microinverters under indoor constant PV power generate CTHD ranging from 6.9% to 13%.

Furthermore, I have shown that the slope for the CTHD profiles for systems under constant PV power was zero whiles; it was positive (increased linearly) for the outdoor study. It has also been established that the CTHD generated by string inverter systems was lower than that for the microinverters. It ranged between 4.5% to 20%. I have shown that the CTHD profiles do not always correlate with the solar radiation profile; thus, the correlation between the CTHD and irradiation is not significant enough to determine its conformity with the grid codes.

3. Impact of system harmonic voltage on the harmonic current generation

I investigated the correlation between the generated harmonic current and the system harmonic voltage of grid-connected PV systems with microinverters and string inverters for varying data points and operating conditions. I have

established that the generated harmonic current of the 5th harmonic order for both microinverter systems and string inverter systems correlate positively with the system harmonic voltage of the studied systems irrespective of system type or operating condition in the low voltage grid systems.

I developed a linear model for the relationship between the harmonic current and the harmonic voltage for the 5th harmonic order of microinverter systems and string inverter systems employed in low voltage grid systems as:

$$I_H = 0.03979 + 0.0064 \; V_H,$$

where the standard deviation was determined to be 0.0011.

I have also ascertained that the relationship between the harmonic current and the harmonic voltage for the 3rd, 7th, 9th and the 11th harmonic orders for both microinverter and string inverter systems connected to the low voltage power network followed no particular predictable trend but was dependent on the pertaining operating condition.

4. Voltage harmonic generation by micro and string inverter systems

Through the experimental results, I have proven that the VTHD, VIHD, the phase voltage, the line voltage and the frequency of the microinverter systems and string inverters are not significantly impacted by the solar radiation and the conditions of the PV system. It was found that the VTHD, VIHD, the phase voltage, the line voltage and the frequency of the microinverter systems and string inverters were within the specified requirement under the studied conditions.

Additionally, I have determined that the voltage harmonics generated by microinverter systems and string inverter systems in low voltage grid systems studied have no significant correlation with the solar radiation profile.

5. Voltage flicker generation

Based on the experimental results, I have established that the performance of microinverters under constant solar irradiation or PV power simulator generates higher severity of short-term flickers compared to their performance in outdoor conditions. It has been proven that the intermittence of solar radiation; hence, intermittent PV power generation does not have any significant correlation with the generation of short-term voltage flickers (Pst) in the power output of microinverters.

3. CONCLUSION AND SUGGESTIONS

In conclusion, experimental analysis has been conducted to determine the power quality performance and compliance with grid codes by different types and scenarios of solar PV grid-connected systems. It has been found that the CTHDs measured for the studied microinverters under the outdoor conditions far exceeded that for the study with the PV simulator for all scenarios and microinverters. The current THD profiles for the scenarios under constant simulated PV power showed a zero slope in the entire study period whiles the outdoor study with the microinverters showed positive slopes.

Microinverters under outdoor conditions generated current total harmonic distortions ranging from 14.3% to 129.5%. However, under indoor conditions, the maximum CTHD was 13%, and the minimum was 6.9% which were virtually constant throughout the entire measurement period. The string inverters comparably generated lower average CTHDs. Except for the SE 3500-ER-01-ITA single-phase string inverter, which generated an average value of 4.65% on one occasion, the recorded CTHDs were all above the 5% specified standard. The days with the highest and non-intermittent solar radiation did not produce the lowest CTHD. Thus, CTHD generation is dependent on the cumulative interaction between the inverter components and the operating conditions available.

The measured power factors for the outdoor studies exhibited varying trends with compliance to the integration requirements. Under the PV simulator, the power factor was almost 100% in conformity with the standards. Thus, the power factor is strongly dependent on the steadiness of solar radiation and remains within the standard limit with irradiations above 400 Wm^{-2}, irrespective of intermittency.

Except for the 5th harmonic order, which showed a positive correlation between the generated harmonic current and the harmonic voltage, all other harmonic orders recorded varying trends for the different inverters and systems studied.

As a recommendation, further studies should be conducted to investigate the interaction of the various grid-connected PV systems and the distribution system during full equipment usage. Long periods of study on the various systems should be conducted and the cumulative effect of multiple systems on the grid investigated. Further work on the performance of other inverter types should be carried out.

4. SUMMARY

PERFORMANCE AND POWER QUALITY EVALUATION OF GRID-CONNECTED SOLAR PHOTOVOLTAIC SYSTEMS

The first section of the study dealt with the comprehensive analysis of microinverters' power output by employing a solar PV power simulator (GUNT equipment), and real modules of different technologies and make (structure). The next was to investigate the power quality output of commercially available microinverters (MaySun-600W-B (China inverter) and the GMI 300 (Holland inverter) microinverters) by employing different modules under outdoor conditions. Investigations were also conducted on large grid-connected single phase string inverters.

The results showed that microinverters' current THDs under the outdoor operating conditions far exceeded the current THDs for the study with the PV simulator for all scenarios and microinverters studied. The current THDs for the studies with all the microinverters under both indoor and outdoor conditions flouted the grid standards. The current THD profiles for the studies with the simulated PV power showed a zero slope for the entire study period, whiles it was positive for the studies under outdoor conditions for the microinverters.

The string inverters comparably generated lower average CTHDs. However, except for the SE 3500-ER-01-ITA single-phase string inverter which generated an average value of 4.65 % on one occasion, the recorded CTHDs were all above the 5% specified standard. Results showed that the inverse rule for the power factor and the CTHD did not hold for all inverters studied under different solar irradiation levels.

The measured power factors for the outdoor studies for both microinverters and string inverters exhibited varying trends with compliance to the integration requirements. Under the indoor study using the PV simulator, the power factor was virtually 100% in conformity with the standard. Thus, the power factor is strongly dependent on the steadiness of solar radiation.

Except for the 5th harmonic order, which presented a positive correlation between the generated harmonic current and the system harmonic voltage irrespective of system, inverter size or type, study conditions, the other harmonic orders showed different correlations for varying inverters and conditions.

7. MOST IMPORTANT PUBLICATIONS RELATED TO THE THESIS

Refereed papers in foreign languages:

1. **Atsu, D.,** Seres, I., Farkas, I. (2021): The state of solar PV and performance analysis of different PV technologies Grid-connected installations in Hungary, Renewable and Sustainable Energy Reviews, Vol. 141, No. 110808, 2021, pp. 1-9. ISSN: 1364-0321, (IF: 12.110*).

2. **Atsu, D.,** Seres, I., Farkas, I. (2019): Comparison of efficiency for different photovoltaic modules, Acta Technologica Agriculturae, Vol. 22, No. 1, pp. 5-11. ISSN 1338-5267. doi: 10.2478/ata-2019-0002.

3. **Atsu, D.,** Seres, I., Farkas, I. (2020): Thermal behaviour analysis of different solar PV modules via thermographic imaging, Journal of Renewable and Sustainable Energy, Vol. 12, No. 1:013503, pp. 1-8., ISSN 1941-7012, doi.org/10.1063/1.5113763. (IF: 1.575*).

4. **Atsu, D.,** Dhaundiyal, A. (2019): Modeling of photovoltaic module using the Matlab, Journal of Natural Resources and Development, Vol. 9, pp. 59-69. ISSN 0719-2452, doi: 10.5027/jnrd.v9i0.06.

5. **Atsu, D.,** Dhaundiyal, A. (2019): Effect of ambient parameters on the temperature distribution of photovoltaic (PV) modules, Resources, Vol. 8 (2), 107. ISSN 2079-9276, doi.org/10.3390/resources8020107.

6. Dhaundiyal, A., **Atsu, D.** (2020): The effect of wind on the temperature distribution of photovoltaic modules. Solar Energy, pp. Vol. 201, 259-267. ISSN: 0038-092X, doi: 10.1016/j.solener.2020.03.012 (IF: 4.608*).

7. **Atsu, D.,** Seres, I., Farkas, I. (2019): Degradation and performance evaluation of PV modules in the tropical climate, Mechanical Engineering Letters, Gödöllő, Hungary, Vol. 19, pp. 33-43., HU ISSN 2060-3789.

8. **Atsu, D.,** Seres, I., Farkas, I. (2019): Measurements of the grid quality for PV inverters, Mechanical Engineering Letters, Gödöllő, Hungary, Vol. 17, pp. 14-21. HU ISSN 2060-3789.

9. **Atsu, D.,** Seres, I., Aghaei, M., Farkas, I. (2020): Analysis of long-term performance and reliability of PV modules under tropical climatic conditions in sub-Saharan, Renewable Energy, Vol. 162, pp. 285-295. ISSN: 0960-1481, doi.org/10.1016/j.renene.2020.08.021 (IF: 6.274*).

10. Farkas I., **Atsu D**.: PEARL PV Hungary, PEARL PV Country Reports, COST Action CA16235, December 12, 2020, University of Twente, The Netherlands, pp. 108-115. ISBN 978-90-365-5107-6, doi: 10.3990/1.9789036551083.

Refereed papers in Hungarian language:

11. Seres, I., **Atsu, D**., Farkas, I. (2020): Fotovillamos modulok teljesítményének degradációja, Magyar energetika, 27: 3 pp. 15-20, 6 p.